BNL-68426

BaF_2 POST-DEPOSITION REACTION PROCESS FOR THICK YBCO FILMS

M. Suenaga, V. F. Solovyov, L. Wu, H. J. Wiesmann, and Y. Zhu

Division of Materials and Chemical Sciences
Energy Sciences and Technology Department
Brookhaven National Laboratory
Upton, NY 11973-5000

INTRODUCTION

The basic processes of the so-called BaF_2 process for the formation of $YBa_2Cu_3O_7$, YBCO, films as well as its advantages over the in situ formation processes are discussed in the previous chapter. The process and the properties of YBCO films by this process were also nicely described in earlier articles by R. Feenstra, et al.[1] Here, we will discuss two pertinent subjects related to fabrication of technologically viable YBCO conductors using this process. These are (1) the growth of thick (>> 1 μm) c-axis-oriented YBCO films and (2) their growth rates. Before the detail discussions of these subjects are given, we first briefly discuss what geometrical structure a YBCO-coated conductor should be. Then, we will provide examples of simple arguments for how thick the YBCO films and how fast their growth rates need to be. Then, the discussions in the following two sections are devoted to: (1) the present understanding of the nucleation and the growth process for YBCO, and why it is so difficult to grow thick c-axis-oriented films (> 3 μm), and (2) our present understanding of the YBCO growth-limiting mechanism and methods to increase the growth rates. The values of critical-current densities J_c in these films are of primary importance for the applications, and the above two subjects are intimately related to the control of J_c of the films. In general, the lower the temperatures of the YBCO formation are the higher the values of J_c of the films.[1,2] Thus, the present discussion is limited to those films which are reacted at ~ 735 °C. This is the lowest temperature at which c-axis-oriented YBCO films (1-3 μm thick) are comfortably grown. It is also well known that the non-c-axis oriented YBCO platelets are extremely detrimental to the values of J_c such that their effects on J_c dwarf essentially all of other microstructural effects which control J_c. Hence, the discussion given below is mainly focused on how to avoid the growth of these crystallites when the films are thick and/or the growth rates are high.

The Structure of the YBCO Conductors

The YBCO conductors are only made in tape shapes since the bi-axially textured YBCO formation is required for attaining high values of J_c for the films. Hence, we expect the structure of the completed YBCO conductors to be a similar one to that of the early Nb_3Sn tapes which were used for a 100-m power transmission cable test.[3] A sketch of the cross section of an expected YBCO tape is shown in Fig. 1 following the geometry of the composite Nb_3Sn conductor. It consists of a central core of a metallic substrate with appropriate buffer layers (not shown in the sketch) and a YBCO layer on each side of the substrate, and then thin (~ 25 – 50 μm) Cu sheets are added for the protection of the superconductor from its accidental transformation to the normal state. The thickness of Cu will depend on the applications and has to be determined for each case. Also, it can be made different on each side so that YBCO layers can be placed in compression when the tape is bent. Additionally, a high strength alloy such as a thin stainless steel tape is added on one side of the tape for mechanical strengthening. This will not be required if a high-strength alloy is used for the substrate for the YBCO layers. All of these components will be soldered to the superconductor after a thin metallic layer such as Ag is deposited on the YBCO surfaces. The thickness of the unreacted Nb core in the Nb_3Sn was only 10 –15 μm thick, yet it was possible to process the tape through the chemical etching of the surface layers and the soldering Cu and stainless tapes onto it without damaging the brittle Nb_3Sn.[3] Thus, one expects that the thickness of the substrate can be as thin as or less than ~ 25 μm as long as wide (>> 10 mm) tapes are processed for the YBCO deposition. After these processes are completed, the composite tapes are slit to desired widths.

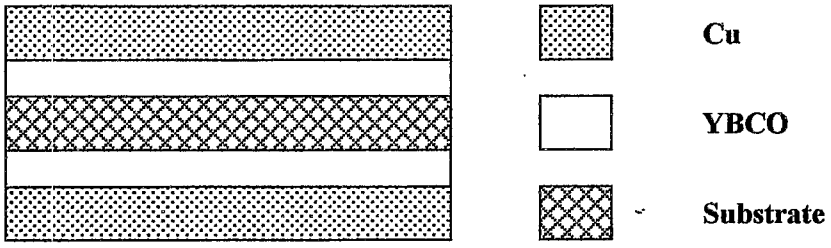

Fig. 1. A schematic sketch of a YBCO conductor cross section.

The Required Thickness of YBCO

Now, what would be the required thickness of YBCO in a tape as shown in Fig. 1? Of course, it will depend on the particular application, but we can obtain a general idea about an approximate required thickness by the following example for the requirement in a power transmission cable. Currently, model cables which have been made and tested for transmission of electrical power employ four layers of Bi(2223)/Ag tapes. If we want to replace them with YBCO tapes, we expect to use only two layers of the conductors (as it was for the Nb_3Sn cable) instead of four. Then, in order to achieve the same critical current I_c in a YBCO cable as for a Bi(2223)/Ag cable, I_c per width of the YBCO tape needs to be ~ 70 A/mm at 77 K under zero magnetic field and since a recent Bi(2223)/Ag tape can carry ~ 100 - 120 A for ~ 3.5 mm width for its critical current. We also assume that the achievable critical-current density, J_c, of a YBCO layer is 10,000 A/mm^2 at 77 K and 0 Tesla. Then, the required total thickness is ~ 7 μm or ~ 3.5 μm per side. If one wants to be conservative or to have an added protection for fault currents, perhaps the thickness should be ~ 5 μm on each side of a tape. Some other applications require higher critical currents.

For example, high-energy particle-accelerator applications demand > 10 μm on both sides while retaining J_c of 10,000 A/mm^2 which is equivalent to ~ 10^5 A/mm^2 at ~ 15 K and 12 T. The above simple example clearly illustrates the necessity that the film thickness be made significantly greater than those currently fabricated (~ 1 μm or less).

The YBCO Growth-Rate Requirement

We estimate the growth rate needed for processing of a YBCO tape with ~ 3.5 μm thick YBCO layers within a practical time by assuming that we need a 1-km tape and use a 10-m-long furnace. We also assume a continuous reel-to-reel process. Finally, we also assume that we need to heat treat this tape for less than a two-week period. This is an arbitrarily chosen period, but commercial Nb_3Sn wires currently require similar periods for their reaction heat treatment. Under these assumed constraints, the rate of the YBCO growth to meet this heat treatment duration is ~ 0.5 nm/s. For some applications, it is possible to heat treat the one sided conductors in a batch process, but this will be more difficult for processing tapes with YBCO on both sides. However, I believe that with some efforts it is possible to design a batch-process reactor for the tapes with YBCO on both sides if the reactor incorporates a subatmospheric pressure process which is described below. In this case, the growth rates of an order of 0.1 nm/s will be sufficient and at this growth rate a 5 μm thick film will be heat treated in less than a day. If such reactors are designed, the requirement for the increased growth rates will be considerably eased.

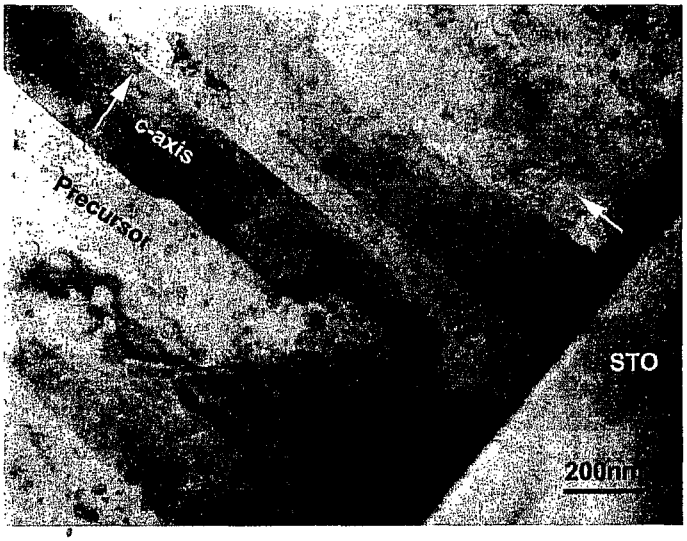

Fig. 2. A cross sectional TEM image of a quenched YBCO film on STO illustrating the growth of the large a-axis oriented YBCO platelets.

The above "required" thickness and growth rate (excluding a batch processing) are substantially greater than those which are being currently achieved, and meeting these requirements simultaneously is a difficult challenge for which we have to address our R and D efforts. Most of the reported thickness and the growth rates are of the order of 1 μm or less and ~ 0.1 nm/s, respectively. The thickest YBCO film, which was made in this process while retaining J_c > 10,000 A/mm^2, was 5-μm-thick films on $SrTiO_3$, STO, substrates.[2] This was synthesized at atmospheric pressure using a very high partial pressure (150 Torr) of H_2O with a growth rate of ~ 0.2 nm/s at 725 °C. However, we feel the use of such a high water partial pressure and an atmospheric pressure process is

impractical as a commercial fabrication process. The main difficulty in achieving the thickness and growth-rate requirements are common, and it is the growth of the non-c-axis-oriented YBCO when the thickness of the YBCO is increased beyond 2 – 3 μm and/or the growth rate exceeds 0.2 - 0.3 nm/s in these films. An example of such undesirable growth of the non-c-axis-oriented YBCO, in this particular case the a-axis crystallites, is shown in Fig. 2 from a film which was grown at a very high growth rate, ~ 1 nm/s. Here, large platelets of the a-axis oriented YBCO are grown out of the substrate while the c-axis-oriented YBCO exists at the substrate but much thinner than the former. When these non-c axis platelets of YBCO grow, the critical currents of the films become disastrously smal due to the highly anisotropic nature of the superconducting current flow in YBCO.

In the following sections, we summarize the results of our studies to the present in the effort to gain understanding of the kinetics of the YBCO nucleation and growth in thick films as well as under the enhanced growth rates. This discussion will be limited to the growth of YBCO on STO from the precursor films which were prepared using electron-beam-evaporation techniques.[4] The early stages of the growth of YBCO on CeO_2 have been previously described[5] and will not be included here. Also, growing thick YBCO films is a major difficulty in the precursor films which are derived from sol gel processes such as the so-called trifluoroacetates (TFA) process. As will be discussed in another chapter, the nature of the difficulty about the growth of the non-c-axis YBCO is similar to what is discussed here. However, there are a number of important differences which exist in the growth processes for YBCO films form the TFA and the physical vapor deposition derived precursors.

THICKNESS: NUCLEATION KINETICS FOR THICK YBCO FILMS

In this section, we will describe our current understanding of the nucleation processes of YBCO from thick precursor films which were deposited onto STO by the electron-beam-evaporation technique.[4] As described earlier,[5] an as-deposited precursor film consists of fine (~ 10 nm) grains of Y, Cu, and BaF_2. Upon heating, the precursor film quickly turns to a mixture of Cu_2O and a (Y,Ba) oxy-fluoride, and then from this mixture the c-axis oriented YBCO is grown on a substrate. The approximate composition of the oxy-fluoride, which plays a key role in the formation of YBCO as well as its nucleation, is $(Y_{0.3}Ba_{0.7})(O_{0.15}F_{0.85})_2$. It is important to note that this phase's crystal structure is identical with BaF_2 and its lattice parameter is very close to that of BaF_2. Thus, when only the standard θ-2θ x-ray diffraction, XRD, measurements are used to study the films, it is often mistakenly reported as BaF_2. Only the combined measurements of its chemical composition and its structural properties by transmission electron microscopy, TEM, techniques can properly identify this new phase. This new oxy-fluoride is clearly identifiable in TEM, particularly in the EDX compositional analysis. However, it is still puzzling how the replacement of Ba and F by Y and O in BaF_2 is accomplished without changing its lattice parameter and crystal structure when the atomic sizes of Y and Ba are significantly different. Thus, the clarification of this puzzle is one of the current subjects of our studies. The mechanism for the c-axis growth of YBCO layers is shown to be the epitaxial precipitation of YBCO onto the existing c-axis-oriented YBCO layer from a thin liquid layer containing Y, Ba, Cu, and O.[5,6] The Y-Ba oxy-fluoride decomposes through the reaction with H_2O at its interface with the liquid releasing F and H to the process gas. At the same time, Cu_2O or CuO, depending on the duration of heat treatment, decomposes into the liquid although the exact mechanism for this is not clear. These decomposition processes provide the necessary cations and oxygen to the liquid and then to the growth of YBCO. Note that this liquid layer only forms on an existing c-axis YBCO layer after a thin (a few tens of nm) layer of YBCO nucleates and covers the substrate, while the growth of

the non-c-axis-oriented YBCO is not associated with this liquid layer. This liquid does not form on the non-c-axis-oriented grains. The details of the growth process are discussed elsewhere.[5] Here, in order to illustrate such a growth process taking place, a cross-sectional TEM image, which was taken from a quenched 3-μm-thick film, is shown in Fig. 3. This shows a thin c-axis-oriented YBCO film on STO and a very thin (~ 7 nm) liquid layer separating the YBCO and the as-yet unreacted precursor. This type of growth is observed when there is no large lateral HF gradients over the film. When large HF gradients exist, the YBCO films appear to grow laterally. This can be seen by purposely designing such gradients over the films[7] or at the edges of the precursor films.[8] It is still unknown whether the liquid is present in these cases.

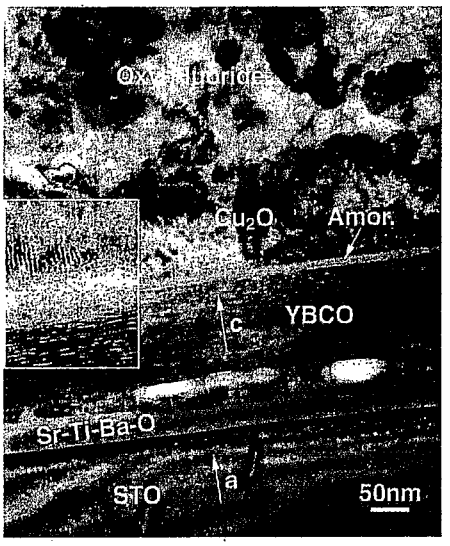

Fig. 3. A cross sectional TEM image showing the liquid (amorphous) layer between the existing YBCO layer and the unreacted precursor from a 3-μm-thick quenched film. The inset image is the enlarge section of the region containing the liquid layer.

From the above description of the YBCO formation process, the basic chemical reaction for the formation of YBCO in the BaF_2 process can be expressed as follows:[5,6]

$$Y + Cu + BaF_2 + O_2 + H_2O \Rightarrow Cu_2O + \text{(Y,Ba) oxy-fluoride} + O_2 + H_2O \quad (1a)$$

$$\Rightarrow YBa_2Cu_3O_{\sim 6.1} + HF\uparrow \quad (1b)$$

Also, as will be discussed below, the basic growth-rate-limiting process is determined by the removal rate of the reaction product HF in Eq. (1b) from the surface of the film into the reaction atmosphere.[7] Furthermore, this reaction is nearly in equilibrium. This is demonstrated in the reversal of the reaction by controlling the partial pressure of HF in the atmosphere. (This was determined by the in situ measurements of the film's conductance during the reaction process.)[9] Hence, the general process for the YBCO growth in the BaF_2 is well understood. However, the precise mechanism of the nucleation of YBCO at the substrate surface is yet unknown. Thus, understanding this nucleation process and finding the means to minimize the non-c-axis-oriented YBCO are particularly important for the fabrication of technologically viable thick YBCO film conductors. This is because the growth of the non-c-axis YBCO becomes prevalent as the thickness of the films increase beyond ~ 2 - 3 μm, and is very detrimental to keeping high values of superconducting

current densities. Thus, in this section, we will summarize the results of our recent study toward the clarification of the mechanism of YBCO nucleation in the BaF_2 process.

In order to understand the nucleation mechanism of YBCO in this process, we heat treated and quenched a set of the precursor films with thicknesses ranging from 1 to 5 μm.[10] All of the specimens were heated in a flowing processing-gas mixture of 100 mTorr of O_2, 25 Torr of H_2O, and N_2 at atmospheric pressure. After 10 min. none of the films showed any indication of YBCO formation by XRD and TEM. At this time, only the Y-Ba oxy-fluoride and Cu_2O was observed and some of the oxy-fluoride grains' (111) planes were aligned with the STO's (001) plane on its surface as shown earlier.[5] The heating duration required for the initiation of the epitaxial nucleation of YBCO at the buried interface, a precursor film and STO, turned out to depend on the film thickness. In a 1-μm-thick film, a thin layer of c-axis oriented YBCO was observed by XRD after 20 min. at 735 °C. However, it took an additional 20 min. of heat treatment for a 3- and 5-μm-thick film to develop a clearly detectable indication of YBCO being present by XRD. However, in the 5-μm film the strong diffraction lines were those belonging to the (*h 0 0*) planes, or the a-axis-oriented grains, while the diffraction lines for a 3-μm film was mostly from the (*0 0 l*) planes as shown earlier.[5]

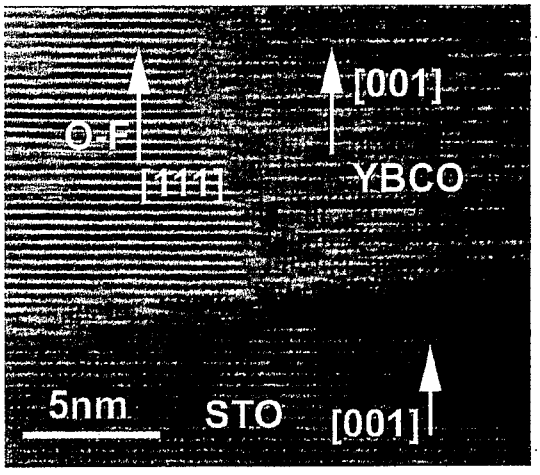

Fig. 4. A cross sectional TEM images showing the YBCO nucleation at STO surface after 20 min. at 735 °C: the (001)- and the (111)-plane-aligned YBCO and the oxy-fluoride, respectively.

A cross-sectional TEM study of the above 1–μm-thick film revealed that the thin (~ 60 nm) c-axis-aligned YBCO layer covered a good fraction of the surface of the substrate, and the remaining areas were occupied by the (111)-plane-aligned oxy-fluoride. In Fig. 4, the alignment of the oxy-fluoride's (111) with STO's (0 0 1) plane is shown adjacent to a c-axis aligned YBCO nucleus. The dimensions of YBCO nuclei in the basal plane were far greater than along the c-direction. This is in accordance with the highly anisotropic growth rates of YBCO, i.e., once it nucleates, its growth in the basal plane was much faster than in the c-axis direction. Energy-dispersive spectroscopy analysis, EDX, shows that the YBCO layers at this stage were still deficient in Cu, and the amount varied significantly from one location to another. The nuclei's composition was in the range of $YBa_2Cu_{1.5\sim2}O_x$.

When the 5–μm-thick specimen was heated for 30 minutes, the unordered and the ordered oxy-fluorides were observed as before.[5,9] The ordered oxy-fluoride has a lattice parameter which is three times that of the unordered one along its c-axis. In addition, what was new in this specimen was the observation of two types of YBCO nuclei which were

oriented with their c-axis perpendicular and parallel to the STO surface, i.e., the c-axis and the a-axis grains, respectively, as shown in Fig. 5 a and b. The amount of these nuclei was so small that XRD measurements did not detect the presence of YBCO. At this moment it is not clear how these two differently oriented nuclei form. After an additional 10 min. of the heat treatment, the a-axis platelets were grown to exhibit strong intensities for the (h 0 0) planes as observed in x-ray diffractograms. Thus, this indicated that once nucleated, the a-axis-oriented nuclei grew extremely rapidly along their a/b- as well as c-directions while the c-axis-oriented grains grew slowly from the substrate along the c-axis as shown in Fig. 2.

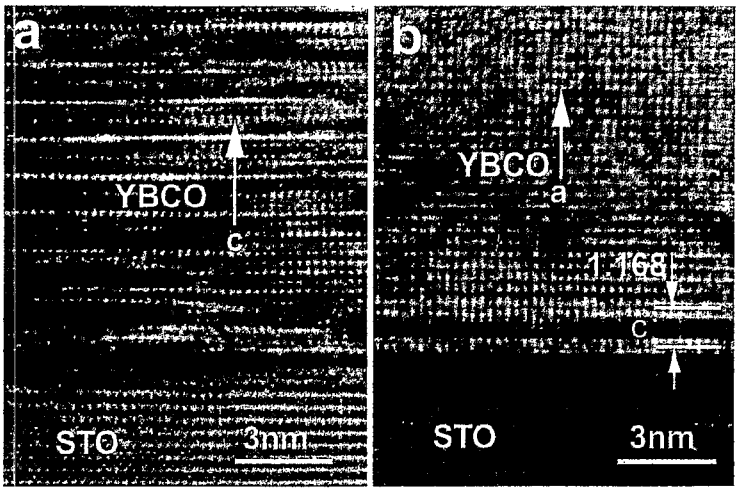

Fig. 5. High resolution TEM images for (a) c-axis and (b) a-axis oriented YBCO nuclei from a 5-μm-thick film heated for 30 min.

The important question, which we need to answer, is what difference in the local conditions at the interface caused the nucleation of differently oriented YBCO nuclei. In attempts to answer this, it is often mentioned that in the thick films the diffusion of H_2O into and of F and H out of the interface region become more difficult as the thickness increases. It is possibly true that the slower diffusion of these species in thick films will delay the nucleation process, but it does not clarify why two types of the nuclei formed. Also, since it was found that the growth rates of the c-axis YBCO are independent of the precursor thickness[2], it is doubtful that the diffusion rates for H_2O and F and H are significantly different for thin and thick films. As mentioned above, the presence of the non-c-axis YBCO platelets in the films are so detrimental that finding the mechanism for and the means to prevent this type of the nucleation is extremely important for the successful fabrication of commercially viable YBCO conductors.

GROWTH KINETICS: ATMOSPHERIC AND SUBATMOSPHERIC PRESSURE PROCESSES

In order to develop a fabrication process for YBCO-coated conductors, it is very important to understand the basic kinetic mechanism(s) for the growth-limiting process in the BaF_2 process. This understanding will help to guide us in developing the required manufacturing process or the reactor designs. In order to accomplish this, we will first treat the growth of YBCO for the process gas flow at atmospheric pressure. Also, we choose a particular set of the conditions, i.e., a small specimen size and a slow gas flow for which an analytical solution is derivable.[10] Then, with similar simplifications, the analysis is

extended for the reaction of a long conductor. Some of the implications from such analyses are discussed relative to processing long lengths of the tapes. We will also discuss a processing method where the heat treatment is carried out in partial vacuum (or subatmospheric pressures).[7,11] It was shown that not only the growth rates could be greatly enhanced in such a processing condition, but also the designs of the reactor operating at subatmospheric pressures could be significantly simplified in comparison with the atmospheric reactor. These findings are very important since in the atmospheric pressure reaction (1) the growth rate of YBCO will be very slow, ~ 0.1 nm/s, unless the gas flow is greatly increased to such high levels that it becomes impractical, and (2) the reactors can be very complicated for long tape fabrications due to the length of the tape, which can be uniformly reacted, is very limited, e.g., a few tens of mm. The advantages in the use of the subatmospheric pressure processing are described in the second part of this section.

Atmospheric-Pressure Process

As described previously, in the atmospheric pressure reactor a mixture of an inert gas, e.g., N_2, and oxygen is humidified and then passed into the reactor at atmospheric pressure. Such a simple design is sufficient to achieve good properties for YBCO films on short buffered tapes or single-crystalline substrates. In order to model the growth kinetics in such a system, we initially assumed that the diffusion of H_2O and/or HF through the unreacted precursor film was the growth-rate-limiting process.[6] However, the analysis of the growth rate based on such an assumption did not yield the linear growth rate with heating time which was experimentally observed.[2] This result and the observations by others (the attempts to process ~ 0.5 m long tapes in the atmospheric reactor resulted in a very inhomogeneous growth from one end of the tape to the other[12]) lead us to seek other rate-limiting causes. One possibility for the occurrence of such an inhomogeniety is due to water vapor starvation of the growing tape. A simple estimate shows that due to very high water vapor pressure and low growth rates, typically found in an atmospheric reactor, the supply of water vapor by diffusion only is more than enough to support stable growth. It is more likely that removal of HF, which is produced as a result of the (Y,Ba) oxy-fluoride decomposition as a part of reaction in Eq. (1b), causes problems with growth inhomogeneity. Thus, with the following simplifying assumptions, we derived an analytical expression for the YBCO growth rate which predicts correctly all of the experimental observations on the growth rate with the heating time, the H_2O partial pressure, and the size of the specimen as variables.[10]

The assumptions used in the model are:

1) The reaction, Eq. (1b), is in a state of dynamic equilibrium at the growth front. If we neglect the spatial variations of $p(H_2O)$ due to high $p(H_2O)$ values, the partial pressure of HF, p_i(HF), at the YBCO-precursor interface is related to the water-vapor partial pressure, $p(H_2O)$, by the equilibrium condition:

$$p_i(\mathrm{HF})/\,[p(\mathrm{H_2O})]^{1/2} = K \qquad (2)$$

where K is the equilibrium constant of the reaction Eq. (1b). If the growth rate is limited by HF removal from the film surface, a simple argument shows that $G \propto p_i(\mathrm{HF})$ but from Eq. (2) $G \propto p(\mathrm{H_2O})^{1/2}$ in agreement with the experimental observation.[3] Our estimates show that the equilibrium constant K is quite small, for instance the equilibrium HF partial pressure is only about 10 mTorr at a typical value of $p(H_2O)$ = 20 Torr.

2) The rate of HF removal is limited by gaseous diffusion in the processing atmosphere. As a consequence HF pressure at the film surface, p_s(HF), can replace the partial pressure at the growth interface, p_i(HF), in Eq. (2). We believe that this is true, at least for films thinner than 5 μm. The most compelling evidence is that the growth rate

does not depend on the precursor film thickness, but depends on lateral width W of the film, that is $G \propto 1/W$. Our interpretation of this observation is that HF flow is determined by the pressure gradient in the gas phase which is approximately $p_s(\mathrm{HF})/W$. Then, the kinetics of growth in the BaF_2 process is reduced to a classic problem of mass transfer from a surface by diffusion and convection of the carrier gas. We treat the case where the gas velocity is quite low. Then, flow is laminar and diffusion is the predominant mechanism of the HF transport from the film surface.

Using the above assumptions, the average YBCO growth rate of a square precursor film with small width W can be expressed as follows:[10]

$$G \approx VDK[p(\mathrm{H_2O})]^{1/2} / kTS \tag{3}$$

where $V = 10^{-22}$ cm^3 is the volume of the YBCO unit cell, k is Boltzmann's constant, T the processing temperature (= 735 °C) and D is the diffusion constant of HF in the processing atmosphere (≈ 2.5 cm^2/s at T = 735 °C *and* p_t = 760 Torr, *the total pressure*). S is a tabulated sample shape factor which also depends on the gas flow rate F. It can be shown that for the case of a small sample, $F >> WD$, $S \approx W$. Note that Eq. (3) appears to predict the growth rate being inversely proportional to temperature contrary to a general intuition about the growth rates. However, since the equilibrium constant K is exponential depends on temperature exponentially, Eq.(3) predicts the temperature dependence correctly, i.e., the higher the temperature the faster the growth.

The case for a long tape can be treated in a similar manner with some additional simplifying assumptions. For example, we have assumed the conductor being a cylinder coated with the precursor film so that an analytical solution for the growth rate can be found. However, an essential parameter in the long-tape case is the HF background pressure, p_b(HF). Since the local growth rate is proportional to the pressure gradient, $G \sim [p_s(\mathrm{HF}) - p_b(\mathrm{HF})]$, the growth slows down considerably when $p_s(\mathrm{HF}) \approx p_b(\mathrm{HF})$ in down stream.[10]

Three factors contribute to the spatial distribution of p_b(HF) along the reactor: (a) HF production by the tape, (b) convection due to carrier gas flow, and (c) gaseous diffusion. In order to simplify the problem the HF concentration gradients in the radial direction were neglected. Combining the three factors above we obtained the following one-dimensional equation:

$$D\, d^2n_b/dx^2 - v dn_b/dx + D\,(n_s - n_b)/S_r = 0 \tag{4}$$

where $n_b(\mathrm{HF}) = p_b(\mathrm{HF})/kT$ is the background HF concentration at a distance x from the "upstream" end of the tape, S_r is the reactor cross-section, $v = F/S_r$ is the carrier gas velocity, F is the gas flow rate, and $n_s(\mathrm{HF}) = p_s(\mathrm{HF})/kT$ is the equilibrium HF concentration at the tape surface, defined by Eq. (2). An analytical solution of Eq. (4) gives the following functional dependence of the growth rate on distance, x:

$$G(x) = G(x=0)e^{-x/\lambda} \tag{5}$$

where $G(x = 0)$ is the growth rate at the upstream end of the cylinder. The parameter λ in Eq. (5) defines the approximate reactor capacity, or maximum tape length, which can be processed in the reactor. λ values depend on the reactor geometry and the gas flow. As assumed in this approximation, if the gas flow is slow, $F << DS_r^{1/2}$, then $\lambda = S_r^{1/2}$, i.e., λ is equal to the reactor radius. An estimate of λ demonstrates that a simple tubular atmospheric-pressure reactor is not suitable for large-scale processing of coated tapes. For example, for our reactor F = 0.20 *l*/min and λ = 70 mm. To react a long tape, much faster gas flow rates are needed, and an exact numerical solution of the corresponding mass

transfer equation is required. However, this simple analysis clearly points out the difficulty of the use of a standard linear-gas-flow reactor for heat treating the long tapes. Such considerations lead to a design of the reactor where the closely spaced in- and out-lets for the gases are needed and these are placed perpendicular to the length of the tape. For a large-scale production facility, this type of the reactor design not only leads to a undesirable complication, but also has other flaws such as a shadowing effect, and requires an excessive amount of the gases needed for the process. Shadowing can be caused by slight local curvatures in the tape or the tape not lying truly parallel to the gas flow. Since the shadowing effect results in nonuniform flow of the gas, it causes nonuniform reactions in some parts of the tape due to nonuniform HF removal rates. If the gas flow is increased to gain high growth rates, an excessive amount of the gases may be needed for the processing long tapes. As described below, in addition to the advantage of having the increased growth rates, the subatmospheric-pressure process can eliminate some of these difficulties by the nature of its process.

Subatmospheric-Pressure Process

In a subatmospheric-pressure reactor a pump is used to force gas transport through the reactor tube. The balance between pumping speed and gas-flow rate defines the absolute pressure in the reactor. The HF diffusion constant in the processing atmosphere depends on the total pressure, p_t, as $D \propto 1/p_t$. It follows from Eq. (3) that the growth rate, G, should depend on p_t and $p(H_2O)$ as:[7]

$$G = A[\,p(H_2O)]^{1/2}/p_t \qquad (6)$$

where A is a constant which can be easily inferred from Eq. (3). We carried out a set of growth runs in a wide range of conditions: total pressure was varied from 0.2 to760 Torr and water-vapor pressure from 10^{-3} to 300 Torr. The samples in each case were 1-μm thick precursor films on 3 × 10 mm^2 substrates, and the processing temperature was 735 °C. The

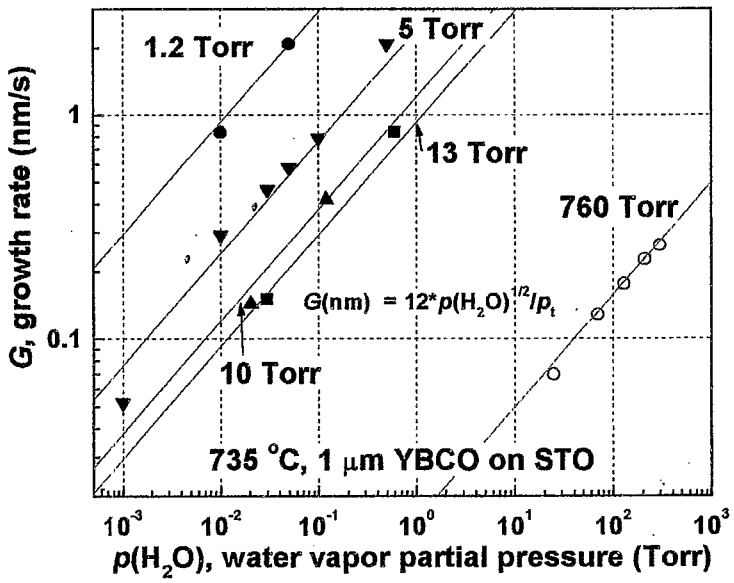

Fig. 6. The growth rates as a function of the partial pressure of H_2O for various total reactor pressures are plotted for the sub-atmospheric BaF_2 process for 1 μm thick films.

results are summarized in Fig. 6 where the growth rate, G, is plotted versus the water-vapor pressure, $p(H_2O)$, for various total-pressure values. Data for the atmospheric reactor are also presented as the curve corresponding to p_t = 760 Torr. Approximations to Eq. (6), where A = 12 and the pressures are in Torr, are shown as solid lines in the figure. It is clear that Eq. (6) well describes the growth kinetics.

It is evident from Fig. 6 that the partial-vacuum reactor allows the achievement of very high growth rates at low total pressures. However, there are important limitations on the utilization of the high growth rates achieved in this process as far as the superconducting current densities are concerned. For 1 μm thick films, we found that for $G > 0.5$ nm/s, YBCO nucleated as a mixture of random and c-axis oriented phases. Stable c-axis growth was observed at $G < 0.2 - 0.3$ nm/s with $J_c(0\ T) \approx 10{,}000$ A/mm^2 and J_c (1T, H||c) $\approx$ 1 to 2×10^3 A/mm^2 at 77 K. Higher values of J_c were measured at lower growth rates. An obvious way to slow down the growth rate is to decrease $p(H_2O)$ and increase p_t. It turns out, however, that $p(H_2O)$ values much less than 10 Torr are detrimental to c-oriented growth in the films much thicker than 1 μm. On the other hand, a partial-vacuum reactor operated at high total pressure is converging towards an atmospheric pressure reactor with all the associated problems outlined in the previous section. Thus, a set of compromise pressures is needed to be determined where a reasonable growth rate G and lengths λ for the uniform YBCO formation, e.g., $G \sim 0.3 - 0.5$ nm/s and $\lambda \sim 20$ - 40 m, respectively, are attainable. One of the possible methods to accomplish this is to grade the total pressure along the reactor tube. For example, for a reel-to-reel system the growth rates at the front end of the tube is made slow by having high H_2O partial and total pressures, but growth rates will be made higher by decreasing the pressures toward the tail end of the reactor. In this way, the c-axis-oriented YBCO is nucleated while the growth rate is controlled to small values at the initial stage of the moving tape. Then, as it moves along the reactor, the pressures are gradually decreased such that the desired higher growth rates are achieved while retaining the c-axis orientation in the YBCO films. Such a reactor requires a careful design of the structure of the tube by a comprehensive study of the gas flow dynamics in the tube. This is one possible approach to solve this difficult problem of the avoidance of the non-c-axis crystallite growth. However, unfortunately, this may require undesirably complicated reactors, and may result in the increased cost for the fabrication of the YBCO conductors. An alternative approach to avoid this complication is to design a tape-holding fixture such that the tapes with YBCO on both sides can be reacted in a batch process. If a such fixture is made the required growth rate can be reduced significantly to more attainable values (e.g. ~ 0.1 nm/s or less). In both cases, some careful engineering reactor designs are needed.

SUMMARY

The BaF_2 process is a very attractive fabrication process for YBCO conductors since it allows the deposition and the formation steps of YBCO films to be separately performed, and it has been demonstrated that the films with high critical current densities can be fabricated on the buffered metallic substrates. However, we still face one major challenge for this process to be made as a commercially viable fabrication method. This is the avoidance of non-c-axis-oriented growth of YBCO when the thickness and the growth rates for the films are increased significantly beyond what are currently achieved. Meeting both the thickness and the growth-rate requirements simultaneously is extremely difficult. One possible way to make the rate requirement reduced is to find winding methods of the tapes in such ways that the both-sided tapes can be reacted in a batch process. Although the winding fixture will be more complicated than a simple dram, I believe that there are ways to construct such fixtures if the subatmospheric-pressure processing is incorporated in the

design for reacting the wide precursor tapes. Then, we are only faced with the problem of growing the c-axis-oriented thick YBCO films. In order to overcome the latter difficulty, we need a detailed understanding of the YBCO nucleation kinetics in thick films under various atmoshperic conditions. Such an understanding is likely to lead to the development of new or modified precursor-deposition methods and/or reaction-heat treatment procedures to facilitate the growth of the thick YBCO layers without the non-c-axis-oriented YBCO growth.

ACKNOWLEGEMENT

The authors are grateful to D. O. Welch and R. Feenstra for stimulating discussions about the subject of this Chapter during the coarse of the study. The work was performed under the auspices of Division of Materials Sciences, Office of Basic Energy Sciences, and Office of Hydrogen and Superconductivity, Office of Energy Efficiency and Renewable Energy, US Department of Energy under contract No. DE-AC02-98CH10886.

REFERENCES

1. R. Feenstra, D.K. Christen, J.D. Budai, S.J. Pennycook, D.P. Norton, H.H. Lowndes, C.D. Klanbunde, and M.D. Galloway, in L. Correra (Ed.), Proc. of Sym. A-1 on High Temp. Supercond. Films at the Internat. Conf. on Adv. Mater. 1991, Strasbury, France, North-Holland, Amsterdam, P. 331; R. Feenstra, T.B. Lindemer, J.D. Bdai, and M.D. Gallorway, J. Appl. Phys. **69**, 6569 (1991).
2. V.F. Solovyov, H.J. Wiesmann, L. Wu, M. Suenaga, and R. Feenstra, IEEE Trans. on Appl. Supercond., **9**, 1467(1999).
3. E.B. Forsyth, Science **242**, 391(1988); J.F. Bussiere, V. Kovachev, C. Klamut, and M. Suenaga, Adv. in Cryog. Engn. **24**, 449 (1977).
4. V.F. Solovyov, H.J. Wiesmann, M. Suenaga and R. Feenstra, Physica C, **309**, 269(1998).
5. L. Wu, V. F. Solovyov, H.J. Wiesmann, Y. Zhu, and M. Suenaga, To be published in Jour. Mater. Res.
6. V.F. Solovyov, H.J. Wiesmann, L. Wu, Y. Zhu, and M. Suenaga, Appl. Phys. Lett. **76**, 1911(2000).
7. V.F. Solovyov, H.J. Wiesmann, L. Wu, Y. Zhu, and M. Suenaga, IEEE trans on Supercond. **11**, 2939(2001).
8. R. Feenstra, a private communication.
9. L. Wu, V. F. Solovyov, H.J. Wiesmann, Y. Zhu, and M. Suenaga. An extended abstract. 2001 International Workshop on Superconductivity, June, 2001, Honolulu, Hawaii.
10. V.F. Solovyov, H.J. Wiesmann, and M. Suenaga, Physica C, **353**, 14 (2001).
11. V.F. Solovyov, H.J. Wiesmann, and M. Suenaga. An extended abstract. 2001 International Workshop on Superconductivity, June, 2001, Honolulu, Hawaii.
12. R. Feenstra, unpublished.